SYSTEM INTERPRETATION OF CAUSALITY MEASURES IN FREQUENCY DOMAIN USED IN EEG ANALYSIS

Tomas Boril, Pavel Sovka

Faculty of Electrical Engineering/Department of Circuit Theory, Czech Technical University in Prague
Technicka 2, 166 27, Prague 6, Czech Republic
phone: + (420) 224 352 291, fax: + (420) 233 339 805, email: boriltom@fel.cvut.cz

ABSTRACT

This paper suggests new measures for the evaluation of an absolute, ratio and relative causal relation in frequency domain in the context of multivariate autoregressive models.

The idea is explained on four synoptic artificial data experiments. In each example, a model without causal connection is presented and then, a causal connection is added. The influence of this modification is analysed and interpreted in the scope of LTI digital filters.

Using the proposed measures, a comparison of results of state-of-the-art frequency domain methods Generalized Partial Directed Coherence (GPDC) and Direct Directed Transfer Function (dDTF) is performed to evaluate their behavior.

The concept is demonstrated on real EEG data of awake resting state of human brain.

1. MOTIVATION

Identification of causal relations in electroencephalography (EEG) is an important problem in the analysis of human brain function during various tasks. It reveals not only the strength of connections but also the direction of information flow among brain structures.

The original idea of Granger causality [7] for two stationary time series compares the prediction error of multivariate autoregressive models (MVAR), modelling the target time series including and excluding the past values of the source time series. If the knowledge of previous values of the source variable helps to predict the current value of the target variable, the variance of the prediction error is lower and we say the source variable has a causal influence on the target variable. Conditional Granger causality [6] extends the idea to three variables in order to distinguish direct relations and indirect ones mediated through the third variable.

The Granger causality concept was used originally in econometrics. In recent years, it has started to be used also on neurophysiological data like functional magnetic resonance imaging, magnetoencephalography and electroencephalography for revealing causal connections among brain structures. A new need for the frequency domain decomposition that would show which rhythms participate in the information flow has arised.

However, the direct transform of Granger causality to the frequency domain for more than two variables, necessary for distinguishing direct and indirect causal connections, encounters problems [4]. New methods DTF [9] and PDC [1] were proposed. Past studies aim to improve the methods to get better behavior on models according to the intuitive expectations, yielding to innovations in the form of dDTF [10] and GPDC [2]. The dDTF features multiplication by a partial coherence, the GPDC adds an extra normalization. The GPDC and dDTF compute only one MVAR model including the source variable, and subsequently, the frequency decomposition of causal relations are calculated from its coefficients. Both methods have been used in numerous studies since their publication, differences of their outputs have been explained intuitively by the nature of diversity of their definitions.

However, an unambiguous definition of frequency meaning of causal relation in the MVAR model is missing. This paper suggests such an explanation using four synoptic artificial models, clearly separating the causal relation. On the basis of this separated relation, absolute, ratio and relative causal measures in frequency domain are proposed. The GPDC and dDTF outputs are compared using the new measures. A new concept of interpretation of GPDC results is presented. The concept is demonstrated on real EEG data of awake resting state of human brain.

2. DEFINITIONS

2.1 Direct Directed Transfer Function (dDTF)

Let us consider process consisting of k stationary variables with zero means (e.g., corresponding to particular channels of EEG data)

$$\mathbf{X}(t) = (X_1(t), X_2(t), \ldots, X_k(t))^T \tag{1}$$

where t stands for the sample index in a discrete time. This process can be fitted into an MVAR model of the order of p

$$\sum_{j=0}^{p} \mathbf{A}(j)\mathbf{X}(t-j) = \mathbf{E}(t) \tag{2}$$

where $\mathbf{A}(j)$ is coefficients matrix of size $k \times k$, weighting the contribution of previous samples delayed by j with respect to the actual sample and $\mathbf{A}(0) = \mathbf{I}$ is identity matrix. $\mathbf{E}(t)$ is a vector of k values of the prediction error, in other words uncorrelated values of white noise with zero mean, calculated as a difference between actual values and predicted values based on the linear combination of p previous samples with the model coefficients $\mathbf{A}(j)$. For the MVAR model coefficients estimation, one can solve Yule-Walker equations obtained as a result of minimization of prediction error variance, or use more robust procedures like Levinson-Wiggins-Robinson (LWR) algorithm based on the idea of maximum entropy, implemented, e.g., in a BioSig toolbox[1]. A detailed comparison of the MVAR estimators was performed in [11] and the LWR method was recommended.

[1] BioSig toolbox for Octave and Matlab available at http://biosig.sourceforge.net/

This model can be transformed into the frequency domain with frequency f, yielding $\mathbf{A}(f)\mathbf{X}(f) = \mathbf{E}(f)$, which can be rewritten as

$$\mathbf{X}(f) = \mathbf{A}^{-1}(f)\mathbf{E}(f) = \mathbf{H}(f)\mathbf{E}(f) \tag{3}$$

where $\mathbf{H}(f)$ is the transfer function of the system. Introducing power spectra

$$\mathbf{S}(f) = \mathbf{H}(f)\mathbf{V}\mathbf{H}^{*}(f) \tag{4}$$

where $*$ denotes transposition and complex conjugate, and $\mathbf{V}$ is the diagonal matrix with variances of noise $\mathbf{E}(f)$. Partial coherence can be then defined

$$\chi_{ij}^2(f) = \frac{M_{ij}^2(f)}{M_{jj}(f)M_{ii}(f)} \tag{5}$$

where $M_{ij}(f)$ is a minor created by removing ith row and jth column of the spectral matrix $\mathbf{S}$. Paper [10] utilized the full frequency DTF (ffDTF)

$$\eta_{ij}^2(f) = \frac{\left|H_{ij}(f)\right|^2}{\sum\limits_f \sum\limits_{m=1}^{k} |H_{im}(f)|^2} \tag{6}$$

to introduce so-called Direct Directed Transfer Function (dDTF)

$$\delta_{ij}(f) = \chi_{ij}(f)\,\eta_{ij}(f) \tag{7}$$

which is a combination of the information from the partial coherence and the information of the direction of influence, which leads to a reliable differentiation of the direct causal connections from the indirect ones. This dDTF is also implemented in the BioSig toolbox mentioned above.

2.2 Generalized Partial Directed Coherence (GPDC)

GPDC is defined in [2] as

$$\mathrm{GPDC}_{ij}(f) = \frac{\frac{1}{\sigma_i}\left|A_{ij}(f)\right|}{\sqrt{\sum\limits_{m=1}^{k}\frac{1}{\sigma_m^2}\left|A_{mj}(f)\right|^2}} \tag{8}$$

where σ_i^2 denotes the variance of noise $E_i(t)$. GPDC is also available in BioSig toolbox.

2.3 Model Order Estimation and Statistical Evaluation

In order to fit real data into the MVAR model, the order of the model p has to be chosen. Akaike Information Criterion (AIC) or Bayesian Information Criterion (BIC) described e.g. in [5] are often used for model order estimation, or one can use an experimental approach published in [3].

Since the causal measures have highly nonlinear relation to the time series data from which they are derived and distributions of their estimators are not well established, [8] proposed an empirical distribution technique using surrogate data. These data are created by random permutations of samples in original channels, which leads to cancellation of causal relations among channels. Causal measures are then estimated from the surrogate data. Repeating this process multiple times, the empirical distribution for the null hypothesis of no causal connection is created.

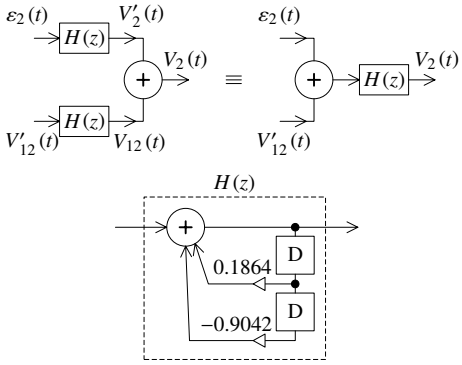

Figure 1: Demonstration of equality in (12) using the LTI superposition principle. Left part: $V_2(t)$ in (12), right part: $V_2(t)$ in (10), bottom part: the common $H(z)$ all-pole filtering used in both left and right part.

3. DEMONSTRATION ON MODEL DATA

3.1 Equation of MVAR model

By reason of clear separation of the causal relation, and thereby its explicit detection, unlike commonly used in literature, a different approach of model data definition is proposed in this paper. Let us consider the following autoregressive time series

$$\begin{aligned} V_1(t) &= \varepsilon_1(t) + 1.5907V_1(t-1) - 0.8133V_1(t-2), \\ V_2'(t) &= \varepsilon_2(t) + 0.1864V_2'(t-1) - 0.9042V_2'(t-2), \end{aligned} \tag{9}$$

$$\begin{aligned} V_{12}'(t) &= a_1V_1(t-1) + a_2V_1(t-2) + \ldots + a_{15}V_1(t-15), \\ V_2(t) &= V_{12}'(t) + \varepsilon_2(t) + 0.1864V_2(t-1) - 0.9042V_2(t-2) \end{aligned} \tag{10}$$

where t stands for the index of a discrete time instance, ε_1 and ε_2 are Gaussian white noises with zero means and unit variances. Variables V_1 and V_2' are single autoregressive signals without any causal relations. These formulas correspond to an all-pole infinite impulse response (IIR) filtering of white noise.

In contrast with V_2', V_2 has an additional causal relation $V_1 \to V_2$ defined in the conformity with MVAR signals with formula $V_{12}'(t)$. The V_{12}' equation performs filtering of V_1 via finite impulse response (FIR) filter of the order of 14 with coefficients $a_1 \ldots a_{15}$ defined for four synoptic cases later.

For the evaluation of the full influence of V_{12}' to V_2, it is necessary to reflect the feedback of the previous samples of V_2 to the actual $V_2(t)$. Let us define

$$V_{12}(t) = V_{12}'(t) + 0.1864V_{12}(t-1) - 0.9042V_{12}(t-2) \tag{11}$$

thus the total causal relation $V_1 \to V_2$ corresponds to V_{12} which is the combination of a FIR filtration and an all-pole IIR filtration.

The final MVAR model consists of the variables V_1 and V_2. Since all filters are LTI systems, the superposition principle can be applied

$$V_2(t) = V_2'(t) + V_{12}(t) \tag{12}$$

(see Fig. 1). Hereby, the causal relation $V_1 \to V_2$ is clearly separated and explained in the frequency domain using V_{12}.

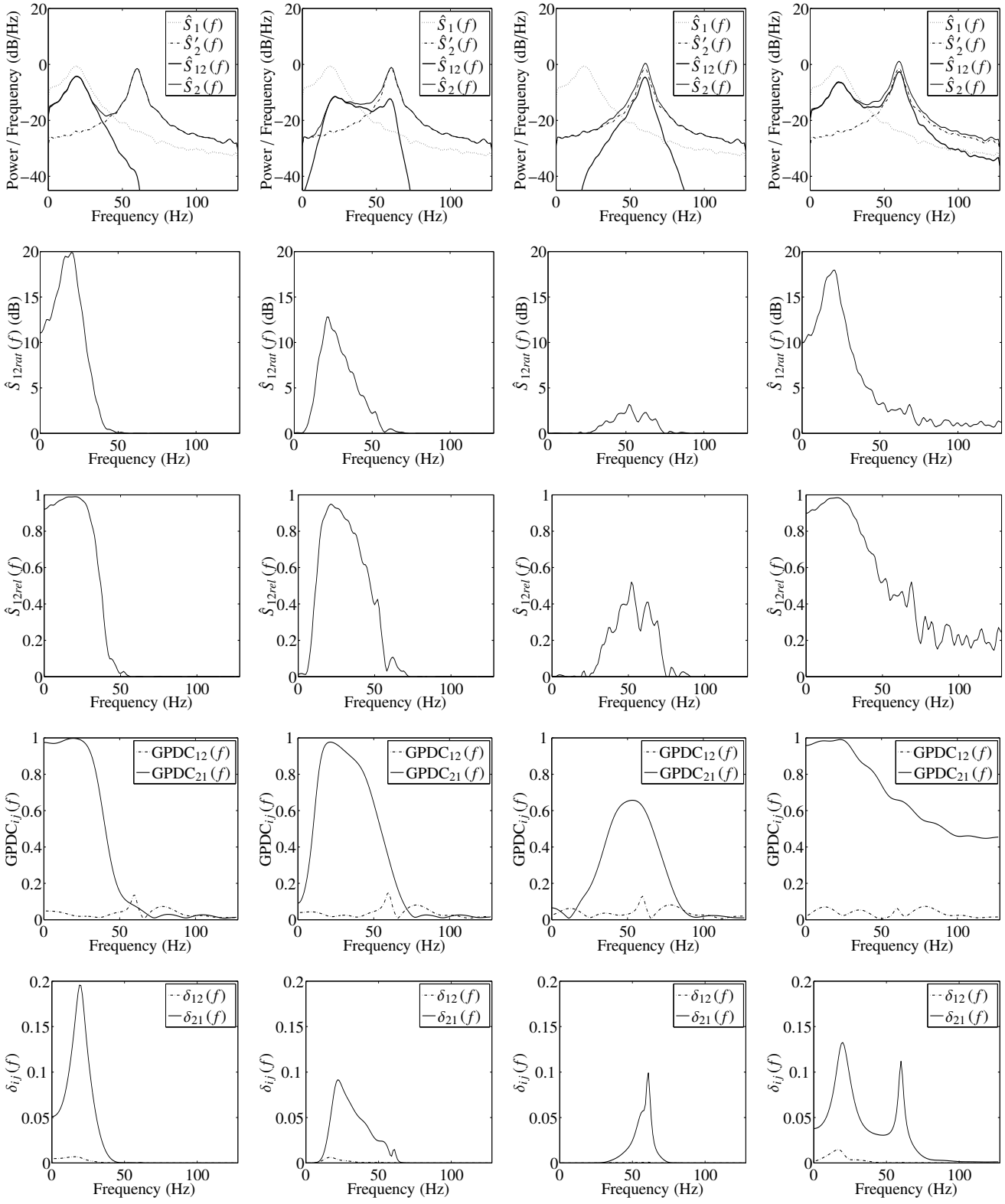

(a) V'_{12}: FIR 10 – 30 Hz (b) V'_{12}: FIR 30 – 50 Hz (c) V'_{12}: FIR 50 – 70 Hz (d) V'_{12}: 1st order highpass FIR

Figure 2: Four models (columns), first row: Welch power spectral density estimate (PSD) of source variable ($\hat{S}_1(f)$), target variable with ($\hat{S}_2(f)$) and without ($\hat{S}'_2(f)$) causal relation $V_1 \to V_2$, the bold line corresponds to PSD of absolute causal relation $\hat{S}_{12}(f)$, second row: ratio causal relation, third row: relative causal relation, fourth and fifth row: GPDC and dDTF analysis of causal relations $V_1 \to V_2$ and $V_2 \to V_1$.

3.2 Model parameters

For demonstration, 7680 samples of the MVAR signals were generated, which corresponds to 30 seconds of two channels with sampling frequency $f_s = 256\,\text{Hz}$. Coefficients of V_1 part in (9) were designed to represent an all-pole resonator (bandpass) with the peak frequency of 20 Hz and bandwidth of 8 Hz, coefficients of V_2' part in (9) feature an all-pole resonator with the peak frequency of 60 Hz and bandwidth of 4 Hz.

Four models with different causal relation connections were created by the choice of coefficients $a_1 \ldots a_{15}$ in (10). In the first three models, these coefficients form an FIR bandpass of the order of 14, designed via the windowing method utilizing Hamming window, specifically with bands $10-30\,\text{Hz}$, $30-50\,\text{Hz}$ and $50-70\,\text{Hz}$. In the last model, only the first two coefficients were set to values 1.19 and -0.5, the rest were set to zero, resulting in a very smooth first order highpass with unit transfer at 40 Hz and a total range from $-3.2\,\text{dB}$ in stopband to $+4.6\,\text{dB}$ in passband.

The Welch power spectral density estimates (PSD) were calculated using Hann window of the size of 128 with a 64 samples overlap, yielding to variable $\hat{S}_1(f)$ corresponding to PSD of V_1 etc.

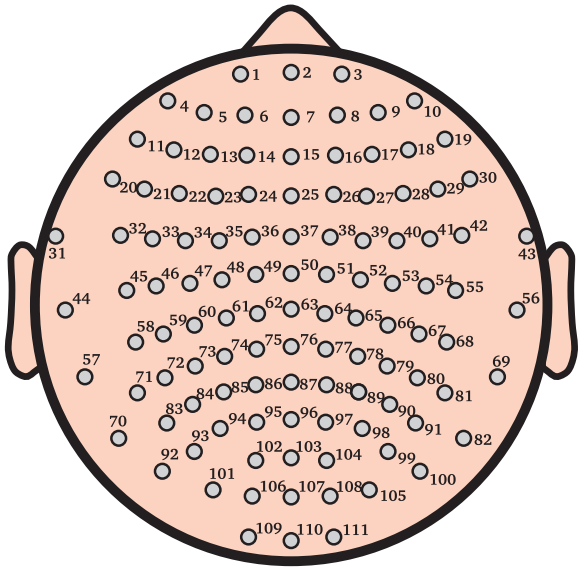

Figure 3: Indexing of 111 scalp EEG electrodes.

3.3 Suggested Criteria

The criteria for the evaluation of the methods performance are as follows.

Absolute causal relation in frequency domain:

$$\hat{S}_{12}(f) = \hat{S}_2(f) - \hat{S}_2'(f) \tag{13}$$

where $\hat{S}_2'(f)$ corresponds to the signals without the causal relation, $\hat{S}_2(f)$ contains the causal relation (see the first row in Fig. 2 where each column corresponds to one of four models).

Ratio causal relation:

$$\hat{S}_{12rat}(f) = \hat{S}_2(f)/\hat{S}_2'(f) \tag{14}$$

is displayed in the second row in Fig. 2.

Relative causal relation:

$$\hat{S}_{12rel}(f) = \left(\hat{S}_2(f) - \hat{S}_2'(f)\right)/\hat{S}_2(f) \tag{15}$$

is in the third row in Fig. 2. Equations (13) and (15) are in the relation

$$\hat{S}_{12}(f) = \hat{S}_{12rel}(f)\,\hat{S}_2(f). \tag{16}$$

The ratio (14) and relative (15) causal relations are given by

$$\hat{S}_{12rat}(f) = \frac{1}{1 - \hat{S}_{12rel}(f)}. \tag{17}$$

The last two rows in Fig. 2 contain GPDC and dDTF measures for both directions of the possible causal relation.

4. EXPERIMENT WITH REAL EEG

The concept of use of previously discussed criteria is demonstrated on experiment with real EEG data to reveal connections among brain centers during an awaked resting state with closed eyes.

The EEG data using 111 scalp electrodes were sampled with $f_s = 256\,\text{Hz}$. Twelve realizations of 30 seconds data segments were used. The electrode positions can be seen in Fig. 3.

Data was fitted into the MVAR model of the order of 15. Because the function $\hat{S}_2'(f)$ is not available for the real data, the following procedure is suggested. First, the GPDC estimator is calculated. The choice of GPDC is explained in the discussion section below. Second, the ratio causality from the GPDC is evaluated in conformity with (17). This procedure is based on the fact that the GPDC results are very similar to our understanding of the relative causality.

The conversion of the GPDC to ratio form is proposed to better distinguish between strong and weak relations. Granger causality is also defined in the ratio form so the results can be interpreted in the same way.

The statistical significance threshold of the results is performed as described in Section 2.3 with 500 permutations of surrogate data using a significance level of 0.05 and the Bonferroni correction. The illustration of the results is given in Fig. 4, the ratio of the causal relation evaluated using the GPDC and the threshold given by surrogate data are depicted. This figure demonstrates a significant relation between electrodes 94 and 12. The alpha rhythm around 10 Hz typical for resting state is visible as the first peak. Other relations were found between electrodes 94 and 72, 98 and 79, and 79 and 12. These results correspond with the assumptions made by physiologists about the EEG activity propagation from the occipital area to the front parts of the brain.

5. DISCUSSION AND CONCLUSIONS

Simulations using modelled data confirm the GPDC results are very similar to our understanding of the relative causality. However, direct use of GPDC (or the relative causality) to reveal causal connections could be misleading because it can show high values even at frequencies where signals have very low power. That is why the absolute value of the power of the causality should be estimated by multiplication of GPDC by PSD of the target variable as defined in (16).

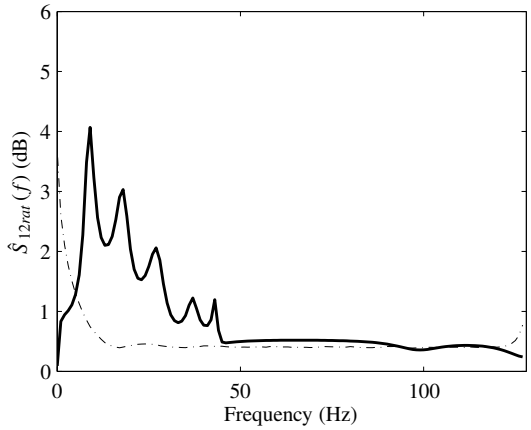

Figure 4: Ratio causality in decibels based on GPDC between electrodes 94 and 12 (the bold line). The first peak corresponds with alpha rhythm around 10 Hz typical for resting state of the brain function. Dot-and-dash line represents significancy threshold, values above the line are significant.

However, in the third artificial model, the causal connection transfers the information from the band around 60 Hz which has a very low power in the source variable. Although the absolute power of the causality seems to be high, it is low in comparison with the power of the target variable in this band. This can be easily seen in the ratio causality in Fig. 2 (second row, third column). The ratio form of causal relation strength calculated from GPDC in conformity with (17) evades this kind of problem.

The definition of dDTF is established by multiplying combination of two autonomous methods, thus it is very hard to interpret the results in such an easy way as with GPDC. The shape of dDTF corresponds partially with the absolute causality because it features only the parts where the signals have a high power, and hence, it could be used directly for revealing causal connections. But in the second model, the shape is very different from the absolute causality. Moreover, the peak values of dDTF are not comparable. While the absolute, ratio and relative causalities show distinctively different values between the second and third model, the dDTF peak values are similar.

Acknowledgements

Research described in this paper has been supported by SGS10/176/OHK3/2T/13 "Brain activity mapping and analysis", Czech Grant Agency under grant No. GD102/08/H008 "Analysis and modelling of biomedical and speech signals" and by research program "Transdisciplinary Research in Biomedical Engineering" No. MSM6840770012 of Czech Technical University in Prague.

REFERENCES

[1] L. A. Baccalá and K. Sameshima. Partial directed coherence: a new concept in neural structure determination. *Biological Cybernetics*, 84:463–474, 2001.

[2] L. A. Baccalá, K. Sameshima, and D. Y. Takahashi. Generalized partial directed coherence. *Proc. of the 15th International Conference on Digital Signal Processing*, pages 163–166, 2007.

[3] T. Bořil. Revealing of relations in EEG via Granger causality. *13th International Student Conference on Electrical Engineering*, pages 1–4, 2009.

[4] Y. Chen, S. L. Bressler, and M. Ding. Frequency decomposition of conditional Granger causality and application to multivariate neural field potential data. *Journal of Neuroscience Methods*, 150(2):228–237, 2006.

[5] M. Ding, Y. Chen, and S. L. Bressler. Granger causality: Basic theory and application to neuroscience. In *Handbook of Time Series Analysis*, pages 437–460. Wiley-VCH Verlag GmbH & Co. KGaA, 2006.

[6] J. Geweke. Measures of conditional linear dependence and feedback between time series. *Journal of the American Statistical Association*, 79(388):907–915, 1984.

[7] C. W. J. Granger. Investigating causal relations by econometric models and cross-spectral methods. *Econometrica*, 37(3):424–38, July 1969.

[8] M. Kamiński, M. Ding, W. A. Truccolo, and S. L. Bressler. Evaluating causal relations in neural systems: Granger causality, directed transfer function and statistical assessment of significance. *Biological cybernetics*, 85(2):145–157, August 2001.

[9] M. Kamiński and K. J. Blinowska. A new method of the description of the information flow in the brain structures. *Biological Cybernetics*, 65(3):203–210, 1991.

[10] A. Korzeniewska, M. Manczak, M. Kaminski, K. J. Blinowska, and S. Kasicki. Determination of information flow direction among brain structures by a modified directed transfer function (dDTF) method. *Journal of Neuroscience Methods*, 125(1-2):195–207, 2003.

[11] A. Schlögl. A comparison of multivariate autoregressive estimators. *Signal Processing*, 86(9):2426–2429, 2006.